JACC: CARDIOVASCULAR IMAGING
VOL. 15, NO. 1, 2022

ORIGINAL RESEARCH

Mitral Annular Dynamics in AF Versus Sinus Rhythm

Novel Insights Into the Mechanism of AFMR

Sébastien Deferm, MD,[a,b,*] Philippe B. Bertrand, MD, PhD,[a,b,*] David Verhaert, MD,[a] Frederik H. Verbrugge, MD, PhD,[b] Jeroen Dauw, MD,[a,b] Kevin Thoelen,[b] Alexander Giesen,[b] Liesbeth Bruckers,[c] Filip Rega, MD, PhD,[d] James D. Thomas, MD,[e] Robert A. Levine, MD,[f] Pieter M. Vandervoort, MD[a,b]

ABSTRACT

OBJECTIVES This study aimed to investigate mitral annular dynamics in atrial fibrillation (AF) and after sinus rhythm restoration, and to assess the relationship between annular dynamics and mitral regurgitation (MR).

BACKGROUND AF can be associated with MR that improves after sinus rhythm restoration. Mechanisms underlying this atrial functional MR (AFMR) are ill-understood and generally attributed to left atrial remodeling.

METHODS Fifty-three patients with persistent AF and normal left ventricular ejection fraction were prospectively examined by means of 3-dimensional transesophageal echocardiography before, immediately after, and 6 weeks after electric cardioversion to sinus rhythm. Annular motion was assessed during AF and in sinus rhythm with the use of 3-dimensional analysis software, and the relationship with MR severity was explored.

RESULTS During AF and immediately after sinus rhythm restoration, the mitral annulus behaved relatively adynamically, with an overall change in annular area of 10.3% (95% CI: 8.7%-11.8%) and 12.2% (95% CI: 10.6%-13.8%), respectively. At follow-up, a significant increase in annular dynamics (19.0%; 95% CI: 17.4%-20.6%; $P < 0.001$) was observed, owing predominantly to an increase in presystolic contraction ($P < 0.001$). The effective regurgitant orifice area decreased from 0.15 cm^2 (0.10-0.23 cm^2) during AF to 0.09 cm^2 (0.05-0.12 cm^2) at follow-up ($P < 0.001$) in the total cohort, and from 0.27 (0.23-0.33) to 0.16 (0.12-0.29) in the subgroup with effective regurgitant orifice area (EROA) ≥0.20 cm^2. The change in presystolic annular motion was the only independent determinant of the decrease in MR severity ($P = 0.027$), by optimizing annular-leaflet imbalance. Patients with more pronounced blunting of presystolic dynamics had a higher EROA ($P < 0.001$), because of a lower total-to-closed leaflet area ratio ($P < 0.001$) at each point in time. This ratio was the strongest independent determinant of AFMR severity (adjusted $P = 0.003$).

CONCLUSIONS Mitral annular dynamics are impaired in AF, with blunted presystolic narrowing that contributes to AFMR. Sinus rhythm restoration allows gradual recovery of presystolic annular dynamics. Improved annular dynamics decrease AFMR severity by optimizing annular-leaflet imbalance, regardless of LA remodeling.
(J Am Coll Cardiol Img 2022;15:1-13) © 2022 Published by Elsevier on behalf of the American College of Cardiology Foundation.

From the [a]Department of Cardiology, Hospital Oost-Limburg, Genk, Belgium; [b]Faculty of Medicine and Life Sciences, Hasselt University, Hasselt, Belgium; [c]Interuniversity Institute for Biostatistics and Statistical Bioinformatics, Data Science Institute, Hasselt University, Hasselt, Belgium; [d]Department of Cardiac Surgery, Cardiovascular Sciences, Leuven University Hospital, Leuven, Belgium; [e]Bluhm Cardiovascular Institute, Department of Cardiology, Northwestern University, Chicago, Illinois, USA; and the [f]Department of Cardiology, Massachusetts General Hospital, Boston, Massachusetts, USA. *Drs Deferm and Bertrand contributed equally to this work.
The authors attest they are in compliance with human studies committees and animal welfare regulations of the authors' institutions and Food and Drug Administration guidelines, including patient consent where appropriate. For more information, visit the Author Center.

Manuscript received April 27, 2021; accepted May 14, 2021.

ISSN 1936-878X/$36.00
https://doi.org/10.1016/j.jcmg.2021.05.019

ABBREVIATIONS AND ACRONYMS

AF = atrial fibrillation

AFMR = atrial functional mitral regurgitation

AP = anteroposterior

EROA = effective regurgitant orifice area

LA = left atrial

LV = left ventricular

MR = mitral regurgitation

Approximately 1 in 10 patients presenting with atrial fibrillation (AF) show evidence of mitral regurgitation (MR) despite structurally normal mitral leaflets and normal left ventricular (LV) systolic function (1-3). Left atrial (LA) and mitral annular dilation—by impeding adequate leaflet coaptation—are generally assumed to be the culprit mechanism of this type of MR (ie, atrial functional MR [AFMR]) (1,4). Successful restoration of sinus rhythm has been shown to effectively reduce AFMR, a finding attributed to reverse LA remodeling in sinus rhythm, with significant decreases in LA and mitral annular dimensions (5).

However, beyond LA remodeling, there is increasing evidence that impaired mitral annular dynamics can contribute to AFMR as well (6-8). The mitral annulus is a complex saddle-shaped 3-dimensional (3D) fibrous structure, which alters configuration throughout the cardiac cycle (9). Specific dynamics of the mitral annulus (anteroposterior [AP] contraction, folding, and deepening of the saddle shape) are known to contribute to leaflet coaptation and valvular competence, and are often impaired in various mitral valve pathologies (10,11). Mitral annular dynamics have not been extensively studied in AF, and their mechanistic contribution to AFMR remains unclear. In addition, it remains unclear if and how sinus rhythm restoration affects the dynamics of the mitral annulus and the resulting mitral valve competence.

The present study hypothesized that differences in mitral annular dynamics between AF versus sinus rhythm have a significant impact on mitral valve competence. To address this, mitral annular dynamics were prospectively studied in patients undergoing electric cardioversion of persistent AF, both during AF, immediately after cardioversion and 6 weeks after cardioversion, all in relation to MR severity.

METHODS

STUDY DESIGN AND POPULATION. Patients admitted for electrical cardioversion of persistent AF (defined according to current guidelines as sustained AF >7 days [12]) at a single tertiary care center (Ziekenhuis Oost-Limburg, Genk, Belgium) were consecutively screened for inclusion from 2018 to 2020. Subjects with MR caused by organic disease (ie, primary MR) or subvalvular leaflet tethering (ie, secondary or "ventricular functional" MR) were excluded before study entry. Additional exclusion criteria were: 1) previous cardiac valve surgery; 2) LV ejection fraction <50%; 3) LV regional wall abnormalities; 4) LV end-diastolic volume index >85 mL/m^2 (men) or 78 mL/m^2 (women) (13); 5) identification of intracardiac thrombi; 6) unsuccessful electric cardioversion to sinus rhythm; and 7) inadequate 3D transesophageal image quality to allow reliable analysis of annular dynamics.

The study complies with the Declaration of Helsinki and was approved by the Institutional Review Board (Ethical Committee, Hospital Oost-Limburg Genk). A written informed consent was obtained from each participant before study inclusion.

IMAGE ACQUISITION. Dedicated 3D transesophageal echocardiography was performed during AF, immediately after electric cardioversion to sinus rhythm (within 2 h), and 6 weeks later in the outpatient clinic. Transthoracic echocardiography was performed immediately after electric cardioversion and at 6-week follow-up. Echocardiographic images were obtained with a commercially available system (EPIQ 7, Philips Medical Systems) equipped with an X5-1 and X7-2t or X8-2t phased-array matrix transducer. The transesophageal study was performed under conscious sedation, ensuring that blood pressure was maintained throughout the examination (mean overall blood pressure during examination 128 ± 23/78 ± 13 mm Hg). 3D mitral valve zoom and full-volume images were acquired from the mid-esophageal view. The region of interest was always set to the smallest possible pyramidal volume including the mitral valve to maximize temporal resolution. The single-beat high-volume-rate protocol was used during AF to avoid stitching artefacts while maintaining adequate frame rate. Otherwise, an electrocardiographically gated acquisition was preferred over 4 consecutive cardiac cycles (overall median 3D frame rate was 35 Hz [IQR: 30-42 Hz]). Median frame rate was similar between AF and sinus rhythm (Sign test: $P = 0.659$).

IMAGE ANALYSIS. Echocardiographic data sets were digitally stored as raw DICOM files (or using a proprietary format) on a secured server and analyzed off-line in their original frame rate with the use of third-party software (Image Arena, TomTec Imaging Systems, Unterschleissheim, Germany). All echocardiographic parameters were measured according to American Society of Echocardiography guidelines (13). LA/LV volumes and ejection fraction were measured with the use of the biplane Simpson

FIGURE 1 **Study Workup**

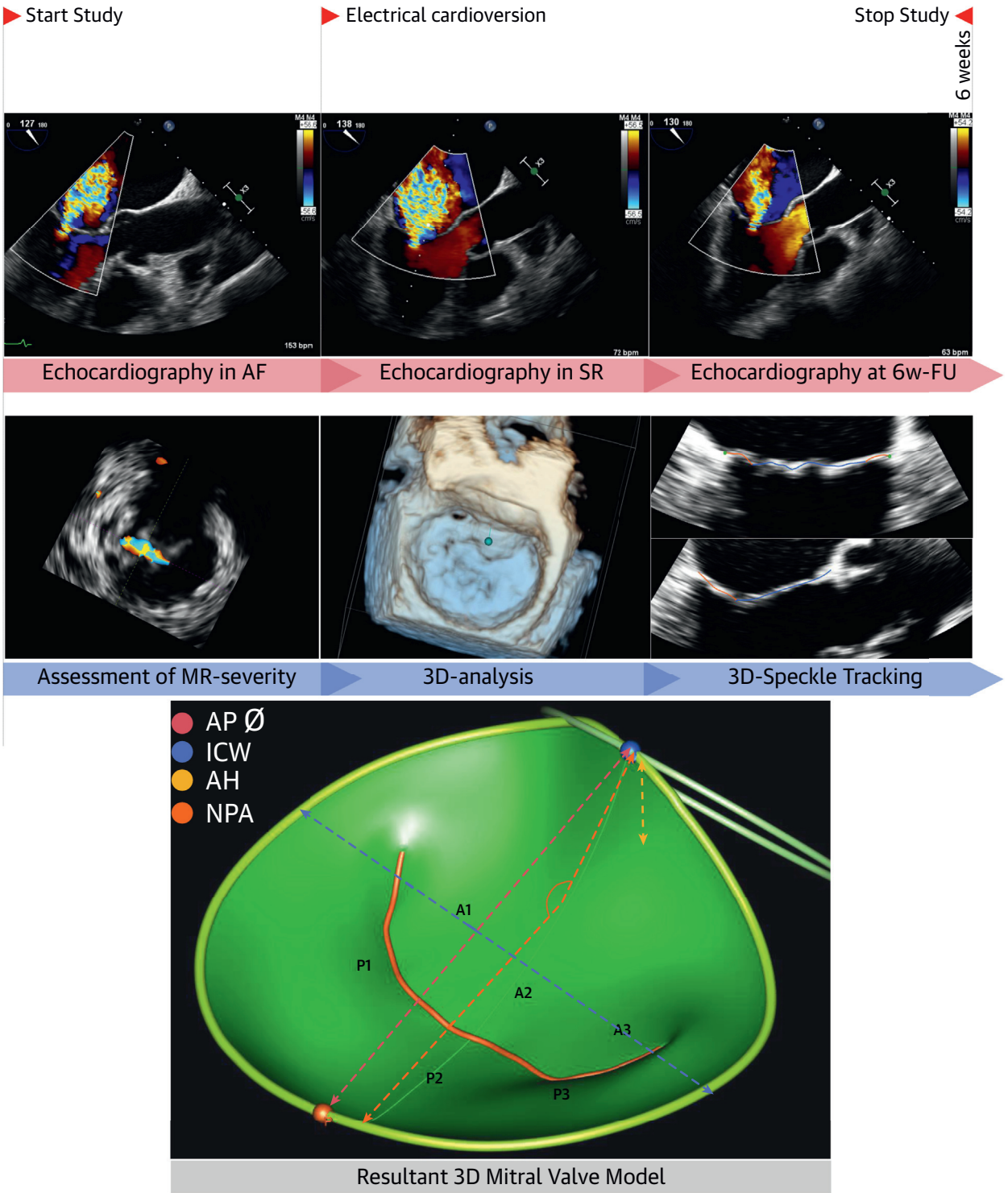

Representative overview of the study methodology. 6wFU = 6-week follow-up; AF = atrial fibrillation; AH = annular height; AP Ø = anteroposterior diameter; ICW = intercommissural width; MR = mitral regurgitation; NPA = nonplanarity angle; SR = sinus rhythm.

method. LV myocardial deformation was assessed in 3 transthoracic apical views by means of off-line speckle-tracking echocardiography (15). MR was assessed with the use of an integrative approach, as recommended (16). The effective orifice area (EROA) was measured by direct 3D planimetry as the cross-sectional area of the largest regurgitant jet vena contracta during systole (ie, 3D vena contracta area). Two orthogonal planes (x and y) were manually cropped parallel through the long axis of the MR jet. A third plane (z), perpendicular to the jet direction was then scanned to identify the cross-sectional area at the level of the vena contracta (17). In case of multiple jets, the imaging plane was oriented through each plane individually (16). In a supplemental analysis, EROA was additionally calculated based on the 2D proximal flow convergence method. In this setting the radius of the proximal isovelocity surface area was always measured at the peak velocity of the continuous-wave Doppler signal through the mitral regurgitant jet. For EROA calculation during AF, the index-beat method was implemented to select the beat with approximately equal preceding and pre-preceding RR interval (14).

Full-volume and mitral valve zoom 3D data sets were digitally imported into the 4D-MV Assessment software package (TomTec Imaging Systems) to assess mitral valve geometry and motion semiautomatically. Briefly, 4 annular points and the leaflet coaptation point were manually marked on the highest-quality data set to initiate annular tracking in mid-systole. A static 3D mitral valve model was then created, after the software automatically defined 80 points around the annular circumference. 3D speckle-tracking algorithms allowed tracking these points throughout systole to create a 3D dynamic mitral valve model. Subsequently, the dynamic data sets were time shifted such that end-systole became the first time point in order to track annular motion during diastole (10).

Annular parameters including annular area, circumference, height, nonplanarity angle, AP diameter, and intercommissural width (ICW)/diameter were determined from the rendered models for each patient (**Figure 1**). The ratio of annular height to ICW was computed to represent the degree of saddle shape (nonplanarity) next to the nonplanarity angle. Seven time points of the cardiac cycle were prespecified for comparative analysis, including mitral valve closure, early systole (aortic valve opening), mid-systole, late systole (frame preceding aortic valve closure), early diastole (maximal early mitral valve opening), mid-diastole, and late diastole (frame preceding mitral valve closure).

The overall change in annular area (total ΔAA) was calculated according the following formula:

$$\text{Total } \Delta AA = \frac{\text{maximum early diastolic value} - \text{value at mitral valve closure}}{\text{maximum early diastolic value}}$$

The presystolic change in annular area (pre-systolic ΔAA) was calculated with the following formula:

$$\text{Presystolic } \Delta AA = \frac{\text{late diastolic value} - \text{value at mitral valve closure}}{\text{late diastolic value}}$$

Finally, the degree of overall leaflet coaptation area (a surrogate marker of valvular competence) in the context of annular dilation, was provided by the ratio of total-to-closed leaflet area:

$$\text{Total to closed leaflet area} = \frac{\text{Total leaflet area in diastole}}{\text{Closed leaflet area in midsystole}}$$

STATISTICAL ANALYSIS. Categoric data are expressed as numbers and percentages and compared with the chi-square test (or Fisher exact test). Continuous variables are expressed as mean ± SD (or 95% CI) if normally distributed, or otherwise by median (IQR, and compared with the use of the independent-samples Student's *t*-test or Mann-Whitney *U* test, respectively. Normality was assessed by means of the Shapiro-Wilk statistic. A repeated-measures mixed model was built to compare annular dynamics during AF, immediate after sinus rhythm restoration, and after 6 weeks, in conjunction with temporal changes within the cardiac cycle. Serial measurements of continuous data were compared with the use of mixed 1-way and mixed 2-way full-factorial analysis of variance, with a random patient effect. Multiple pairwise comparisons were always interpreted with the post hoc Tukey correction. Longitudinal changes in indices of MR severity were examined by the Friedman test with post hoc Sign test. Univariate and multivariate linear regression analysis was performed to determine clinical and echocardiographic predictors of MR severity. Variables with a significance value of $P \leq 0.10$ on univariate analysis were subsequently entered in the multivariate model. Statistical significance was always set at a 2-tailed probability level of <0.05. Statistics were performed with the use of Stata version 16.1 (StataCorp) and SAS JMP Pro 15.2.0 (Statistical Analysis Software,).

RESULTS

BASELINE CHARACTERISTICS OF THE STUDY POPULATION. Sixty patients were considered for study inclusion, of which 7 were excluded because of insufficient image quality. Baseline patient and echocardiographic characteristics for the final study population (n = 53) are summarized in **Table 1**, dichotomized by baseline EROA ≥0.20 cm². Mean age was 69 ± 1 year, and 15 patients (28.3%) were women. Baseline demographics and antiarrhythmic therapy were similar between EROA ≥0.20 cm² and EROA <0.20 cm². Mid-systolic indexed annular area was 6.0 ± 0.9 cm²/m², in line with large AP and transverse diameters. Follow-up was complete in all patients with a median of 52 days (IQR: 47-56 days) between index examination and repeated echocardiography.

MITRAL ANNULAR DYNAMICS DURING AF AND AFTER SINUS RHYTHM RESTORATION. Cyclic changes in annular geometry in AF, in acutely restored sinus rhythm, and after 6 weeks are displayed in **Figure 2**. Pairwise comparisons for annular measurements at different stages of the cardiac cycle in AF, acutely restored sinus rhythm, and 6-week follow-up are presented in Supplemental Table 1.

In persistent AF (**Figure 2**, red curve) and immediately after sinus rhythm restoration (**Figure 2**, green curve), the mitral annulus behaved relatively adynamically, with an overall change in annular area (total ΔAA) of only 10.3% (95% CI: 8.7%-11.8%) and 12.2% (95% CI: 10.6%-13.8%), respectively ($P = 0.087$ for the difference between AF and sinus rhythm). In contrast, at 6-week follow-up (**Figure 2**, blue curve), total ΔAA was 19.0% (95% CI: 17.4%-20.6%; $P < 0.001$ for difference with AF and early sinus rhythm). The most prominent difference in annular narrowing occurred in late diastole (ie, following atrial contraction) with a presystolic ΔAA of 4.8% (95% CI: 3.2%-6.3%) in AF, 5.9% (95% CI: 4.3%-7.4%) in early sinus rhythm, compared with 11.8% (95% CI: 10.2%-13.3%) after 6 weeks ($P = 0.395$ for the difference between AF and early sinus; $P < 0.001$ for the difference between both and 6-week follow-up). This prominent late diastolic annular contraction at follow-up resulted in a significantly smaller annular area and AP valve dimension before the onset of systole compared with AF or early sinus rhythm—a difference in mitral annular area which was maintained throughout systole.

Annular folding (decrease in nonplanarity angle) and deepening of the saddle shape (increase in ratio of annular height to intercommissural width) occurred from mid-diastole through early and mid-systole in both AF and early sinus rhythm. The relative dynamics of folding and saddle deepening were more pronounced at 6 weeks after cardioversion (**Figure 2**), yet the absolute values at each phase of the cardiac cycle were similar for AF, early sinus rhythm, and 6-week follow-up (P = NS for all).

DETERMINANTS OF CHANGES IN MR SEVERITY AFTER ELECTRIC CARDIOVERSION FOR AF. At baseline (during persistent AF), median EROA was 0.15 cm² (IQR: 0.10-0.23 cm²). Early sinus restoration only marginally affected MR severity, whereas at 6-week follow-up a prominent decrease in MR severity was

TABLE 1 Baseline Patient and Echocardiographic Variables for the Study Population, Dichotomized by EROA ≥0.20 cm²

	All Subjects (N = 53)	EROA ≥0.20 cm² (n = 15)	EROA <0.20 cm² (n = 38)	*P* Value
Clinical parameters				
Age, y	69 ± 10	69 ± 8	69 ± 10	0.873
Female	15 (28.3)	9 (60.0)	29 (76.3)	0.235
BSA, m²	2.00 ± 0.22	2.00 ± 0.20	2.00 ± 0.23	0.969
BMI, kg/m²	29.1 ± 5.0	30.0 ± 4.5	28.7 ± 5.2	0.407
Obesity	22 (41.5)	7 (46.7)	15 (39.5)	0.632
Hypertension	35 (66.0)	12 (80.0)	23 (60.5)	0.177
Diabetes	4 (7.6)	2 (13.3)	2 (5.3)	0.568
Dyslipidemia	32 (60.4)	10 (66.7)	22 (57.9)	0.556
Drug therapy at admission				
Beta-blocker	26 (49.1)	6 (40.0)	20 (52.6)	0.407
Class III antiarrhythmic	4 (7.5)	1 (6.7)	3 (7.9)	1.000
Class Ic antiarrhythmic	2 (3.8)	1 (6.7)	1 (2.6)	0.490
ACE-I or ARB	21 (39.6)	6 (40.0)	15 (39.5)	0.972
MRA	3 (5.7)	2 (13.3)	1 (2.6)	0.190
MR severity				
MR EROA, cm²	0.15 (0.10-0.23)	0.27 (0.23-0.33)	0.12 (0.09-0.15)	**<0.001**
LV and LA indices[a]				
LVEF, %	53 ± 3	52 ± 3	53 ± 3	0.669
LVEDVi, mL/m²	61 ± 10	62 ± 12	60 ± 10	0.535
LVESVi, mL/m²	28 ± 6	28 ± 9	28 ± 4	0.765
LV GLS, %	−17 ± 2	−16 ± 3	−17 ± 2	0.444
LV GCS, %	−24 ± 3	−23 ± 3	−24 ± 3	0.311
E, m/s	0.8 ± 0.2	0.9 ± 0.2	0.7 ± 0.2	**0.037**
E/A, abs	2.9 ± 1.4	3.5 ± 1.5	2.3 ± 1.0	**0.001**
E/e′ mean, abs	11.1 ± 4.5	12.6 ± 5.0	10.5 ± 4.3	0.149
LAVI, mL/m²	51 (44-61)	57 (43-60)	50 (44-64)	0.618

Values are mean ± SD, median (IQR), or n (%). Significant *P* values are indicated in **bold**. [a]Measured in sinus rhythm at baseline.

AAi = annular area indexed for body surface area; ACE-I = angiotensin-converting enzyme inhibitor; AH = annular height; AH/ICW = annular height divided by intercommissural width; AP Ø = anteroposterior diameter; ARB = angiotensin receptor blocker; AF = atrial fibrillation; BSA = body surface area; BMI = body mass index; EROA = effective regurgitant orifice area; ICW = intercommissural width; LA = left atrial; LAVI = left atrial volume index; LV = left ventricular; LVEDVi = left ventricular end-diastolic volume indexed for body surface area; LVEF = left ventricular ejection fraction; LVESVi = left ventricular end-systolic volume indexed for body surface area; LV GCS = left ventricular global circumferential strain; LV GLS = left ventricular global longitudinal strain; MR = mitral regurgitation; MRA = mineralocorticoid receptor antagonist.

FIGURE 2 Annular Dynamics During AF, After Sinus Rhythm, and at Follow-Up

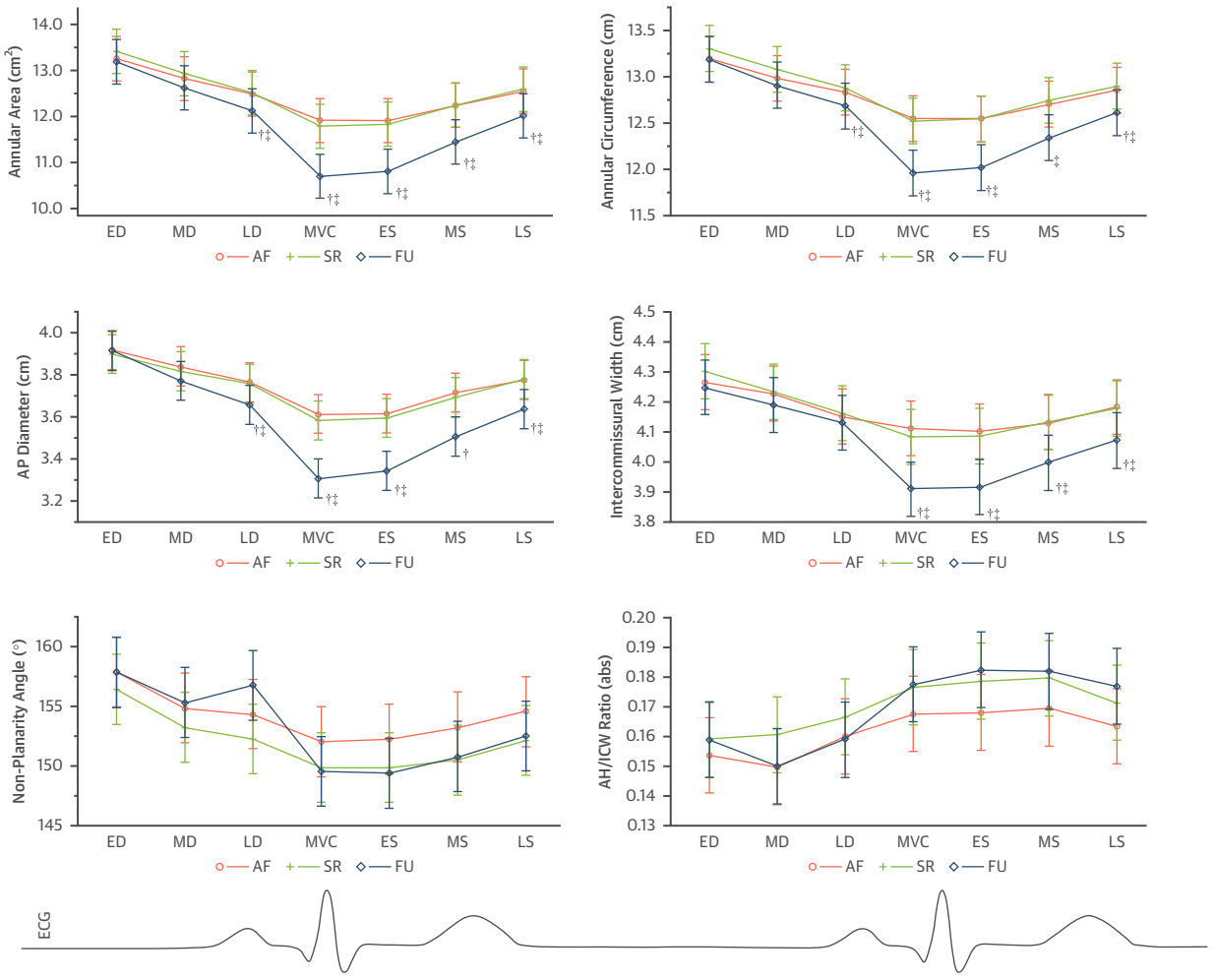

Least squares means plots showing phasic changes in annular area, circumference, anteroposterior diameter, intercommissural width, and indices of annular saddle-shape during AF **(red)**, immediate after sinus rhythm (SR) restoration **(green)**, and at 6-week follow-up (FU) **(blue)**. Presystolic annular dynamics were notably larger at 6-week FU. Data are presented as mean ± 95% CI. ECG = electrocardiography; ED = early diastole; ES = early systole; MS = mid-systole; MD = mid-diastole; LD = late diastole; LS = late systole; other abbreviations as in Figure 1. †$P < 0.05$ vs AF; ‡$P < 0.05$ vs SR.

observed ($P < 0.001$ compared with AF and acutely restored sinus rhythm). Table 2 summarizes the longitudinal changes in MR severity following electric cardioversion to sinus rhythm, along with changes in LV size and function, LA size, and mitral annular measurements. Mitral annular dynamics throughout the cardiac cycle, and the resulting mid-systolic annular measurements, significantly improved after 6 weeks compared with baseline and early after sinus restoration ($P < 0.001$ for all). In multivariable regression modeling for the reduction in MR severity at 6-week follow-up, the absolute improvement in presystolic mitral annular dynamics 6 weeks after cardioversion was most strongly associated with the absolute decrease in EROA (Table 3). The increase in presystolic dynamics at 6 weeks was paralleled by a significantly increase in the total-to-closed leaflet area ratio ($P < 0.001$, compared with baseline) (Table 2), which correlated with EROA, as measured by the 3D vena contracta area ($R^2 = 0.55$; $P < 0.001$) (Supplemental Figure 1) and 2D proximal flow convergence method ($R^2 = 0.53$; $P < 0.001$). In multivariable linear regression analysis the total-to-closure leaflet area ratio was the most important determinant of EROA (Table 4) in AFMR.

TABLE 2 Longitudinal Change in MR Severity, LV, LA and Mitral Annular Indices

	AF	Sinus Rhythm (Acute)	Follow-Up	*P* Value
Blood pressure				
Systolic, mm Hg	131 (125 to 135)	114 (109 to 119)[a]	147 (139 to 152)[a,b]	**<0.001**
Diastolic, mm Hg	83 (79 to 86)	72 (68 to 75)[a]	79 (74 to 82)[b]	**<0.001**
LV and LA indices				
LVEF, %	-	53 (52 to 53)	54 (53 to 54)	**0.010**
LV GLS, %	-	−17 (−18 to −16)	−17 (−18 to −17)	0.137
LV GCS, %	-	−24 (−25 to −23)	−24 (−25 to −23)	0.607
LAVI mL/m^2	-	51 (44 to 61)	50 (44 to 58)	0.053
PALS, %	-	12.2 (10.1 to 15.1)	16.4 (12.7 to 20.6)	**<0.001**
PACS, %	-	2.4 (0.9 to 5.4)	6.4 (4.4 to 8.1)	**<0.001**
Reservoir strain rate, s^{-1}	-	0.47 (0.41 to 0.64)	0.61 (0.51 to 0.69)	0.053
Pump strain rate, s^{-1}	-	−0.27 (−0.49 to −0.11)	−0.60 (−0.88 to −0.45)	**<0.001**
Static annular measurements				
Annular area in mid-systole, cm^2	12.2 (11.7 to 12.7)	12.3 (11.8 to 12.7)	11.5 (11.0 to 12.0)[a,b]	**<0.001**
NPA in mid-systole, degrees	153 (150 to 156)	150 (147 to 153)	151 (148 to 154)	**0.036**
AH/ICW in mid-systole, abs	0.17 (0.16 to 0.18)	0.18 (0.17 to 0.19)	0.18 (0.17 to 0.20)	0.054
Dynamic annular measurements				
Presystolic ΔAA, %	4.8 (3.2 to 6.3)	5.9 (4.3 to 7.4)	11.8 (10.2 to 13.3)[a,b]	**<0.001**
Total ΔAA, %	10.3 (8.7 to 11.8)	12.2 (10.6 to 13.8)	19.0 (17.4 to 20.6)[a,b]	**<0.001**
Total-to-closure ratio, abs	1.09 (1.06 to 1.12)	1.08 (1.05 to 1.11)	1.15 (1.12 to 1.18)[a,b]	**<0.001**
MR severity				
EROA, cm^2	0.15 (0.10 to 0.23)	0.14 (0.10 to 0.22)[a]	0.09 (0.05 to 0.12)[a,b]	**<0.001**
Subgroup EROA ≥0.20 cm^2	0.27 (0.23 to 0.33)	0.24 (0.22 to 0.31)[a]	0.16 (0.12 to 0.29)[a,b]	**<0.001**
Subgroup EROA <0.20 cm^2	0.12 (0.09 to 0.15)	0.12 (0.08 to 0.14)[a]	0.07 (0.05 to 0.09)[a,b]	**<0.001**

Values are mean (95% CI) and compared by means of the paired Student's *t*-test or mixed 1-way analysis of variance (ANOVA) with random patient effect. Nonnormally distributed continuous variables are presented as median (IQR) and compared by means of Friedman ANOVA and post hoc Sign test. Significant *P* values are indicated in bold. [a]$P < 0.05$ vs AF. [b]$P < 0.05$ vs sinus rhythm.

ΔAA = change in annular area; PACS = peak atrial contractile strain; PALS = peak atrial longitudinal reservoir strain; other abbreviations as in Table 1.

ANNULAR DYNAMICS IN THE EROA ≥0.20 cm^2 SUBGROUP. Fifteen patients (28%) had significant AFMR (EROA ≥0.20 cm^2) at baseline. Akin to the overall the study population, presystolic annular narrowing was abolished during persistent AF and immediately after sinus rhythm restoration, with significant recovery at 6 weeks (Supplemental Figure 3). Compared with the subgroup with EROA <0.20 cm^2, the strength of presystolic annular contraction was significantly lower at each point in time (**Figure 3A**). Nevertheless, the recovery in presystolic annular dynamics at 6 weeks was even larger with EROA ≥0.20 cm^2, paralleling a large increase in the total-to-closed leaflet area with significant effect on AFMR severity (Figure). The correlation between the total-to-closed leaflet area ratio, as a measure for leaflet coaptation, and EROA remained valid in the subgroup with EROA ≥0.20 cm^2 ($R^2 = 0.59$).

IMPACT OF RECURRENT AF ON MITRAL ANNULAR DYNAMICS. Recurrent AF occurred in 17 patients (28%) before the 6-week follow-up and was still present in 8 of the 17 patients during the repeated echocardiography. Of note, when subjects with intermittent AF recurrence (n = 17) were excluded, the observed differences in presystolic annular dynamics between follow-up and baseline were even more pronounced (presystolic ΔAA 13.5% (95% CI: 11.7%-15.3%) vs 5.3% (95% CI: 3.5%-7.1%) in AF and 6.2% (95% CI: 4.4%-8.0%) in sinus rhythm; $P <$ 0.001).Vice-versa, presystolic annular narrowing was significantly worse in patients with AF recurrence (n = 17) compared with patients without recurrence (n = 36) at follow-up (presystolic ΔAA at follow-up 8.1% (95% CI: 5.5%-10.7%) vs 13.5% (95% CI: 11.7%-15.3%); $P = 0.005$). Supplemental Figure 2 displays phasic changes in annular area during AF, sinus rhythm, and at follow-up, when dichotomizing patients with and without recurrence of persistent AF before 6-wk follow-up.

REPRODUCIBILITY. Reproducibility of all annular measurements was tested blind in a random sample of 12 patients. The intraclass correlation coefficients for intra-observer and interobserver variability are presented in Supplemental Table 2 and showed overall good agreement.

TABLE 3 Determinants of Absolute Change in EROA From Baseline (AF) to Follow-Up

	Univariate Analysis		Multivariate Analysis		
	Std β	*P* Value	Nonstd β (95% CI)	Std β	*P* Value
Clinical parameters					
Δ BP systolic, mm Hg	−0.085	0.678			
Δ BP diastolic, mm Hg	0.009	0.966			
Δ Heart rate, beats/min	0.245	0.113			
LV and LA indices[a]					
Δ LVEDVi, mL/m^2	0.120	0.455			
Δ LVEF, %	−0.300	**0.056**	−0.006 (−0.012 to 0.001)	−0.261	0.083
Δ LV GLS, %	0.149	0.372			
Δ LV GCS, %	0.263	0.111			
Δ LAVI, mL/m^2	0.109	0.486			
Δ PALS, %	−0.266	0.135			
Δ PACS, %	0.032	0.895			
Δ Reservoir strain rate, s^{-1}	−0.099	0.585			
Δ Pump strain rate, s^{-1}	−0.176	0.379			
Dynamic annular measurements					
Δ Presystolic dynamics, %	−0.568	**<0.001**	−0.499 (−0.938 to −0.060)	−0.463	**0.027**
Δ Total annular dynamics, %	−0.324	**0.034**	0.174 (−0.205 to 0.554)	0.188	0.357
Static annular measurements					
Δ Annular area in early diastole, cm^2	0.102	0.515			
Δ Annular area in mid-systole, cm^2	0.423	**0.005**	0.025 (−0.027 to 0.078)	0.286	0.336
Δ NPA in mid-systole, degrees	−0.299	**0.052**	−0.001 (−0.003 to 0.002)	−0.096	0.613
Δ AH/ICW ratio in mid-systole, abs	0.297	**0.053**	0.049 (−0.501 to 0.599)	0.036	0.857
Leaflet coaptation					
Δ Total-to-closed leaflet ratio, abs	−0.366	**0.016**	−0.048 (−0.312 to 0.215)	0.090	0.715

Possible predictors are presented with their corresponding regression coefficients and *P* values. Variables with $P < 0.10$ in univariate linear regression were subsequently entered into the multivariable linear regression model. Multicollinearity was always verified. Mean variance inflation factor was 2.50. Significant *P* values are indicated in **bold**.
[a]Measured in sinus rhythm at baseline.

Δ = change from baseline to follow-up; std = standardized; nonstd = nonstandardized; other abbreviations as in Table 1.

DISCUSSION

This study prospectively investigated differences in mitral annular dynamics in AF versus sinus rhythm, and the impact of changes in annular dynamics on mitral valve competence and AFMR. The key findings of this study (**Central Illustration**) are that: 1) mitral annular dynamics are decreased during persistent AF and immediately after cardioversion, particularly affecting annular narrowing in late diastole (presystolic phase); 2) enhanced presystolic annular narrowing in sinus rhythm improves valve coaptation throughout systole and decreases MR severity regardless of global LA size; and 3) the balance between the total mitral leaflet area and the minimal closed leaflet area needed during systole is a key determinant for the occurrence of AFMR in patients with persistent AF.

MITRAL ANNULAR DYNAMICS IN AF. The motion of the fibrous mitral annulus is passively imposed by contraction/relaxation of adjacent LA/LV musculature through its atrioventricular roots (9). This annular and atrioventricular coupling is a crucial component of normal mitral valve functioning. Presystolic atrial contraction reduces annular area and facilitates leaflet coaptation when valve-closing forces are yet submaximal during early LV pressure rise (10,18). In addition, presystolic and systolic saddle-shape deepening—reaching its deepest saddle shape in mid-systole (10,18)—can blunt stresses imposed on the leaflets during systole (19). As such, mitral annular dynamics play an important role in ensuring adequate mitral valve closure at minimal leaflet stress.

During AF, annular dynamics become predominantly systolic, with loss of the atrial contribution to the annular motion that might adversely affect valvular competence. Experimentally induced loss of atrial systole dissipates the presystolic annular contraction and saddle-shape deepening, and delays mitral valve closure in sheep (20-23). Similar observations of decreased presystolic contraction have been described in patients presenting with AF and have been suggested to be associated with to the presence of MR (6,24).

On top of reinforcing these previous observations with prospectively collected longitudinal 3D transesophageal

TABLE 4 Determinants of EROA in Persistent AF

	Univariate Analysis		Multivariate Analysis		
	Std β	*P* Value	Unstd β (95% CI)	Std β	*P* Value
LV and LA indices					
LVEDVi, mL	0.078	0.630			
LVEF, %	−0.105	0.513			
LV GLS, %	0.157	0.347			
LV GCS, %	0.204	0.220			
LAVI, mL/m^2	0.129	0.410			
PALS, %	−0.267	0.133			
PACS, %	−0.119	0.590			
Reservoir strain rate, s^{-1}	−0.253	0.156			
Pump strain rate, s^{-1}	0.314	**0.075**	0.100 (−0.051 to 0.252)	0.203	0.186
Dynamic annular measurements					
Presystolic ΔAA, %	−0.455	**0.002**	−0.101 (−1.326 to 1.124)	−0.043	0.867
Total ΔAA, %	−0.345	**0.023**	0.262 (−0.826 to 1.350)	0.111	0.625
Static annular measurements					
Annular area in early diastole, cm^2	0.254	0.100			
Annular area in mid-systole, cm^2	0.306	**0.046**	−0.001 (−0.024 to 0.022)	−0.014	0.946
NPA in mid-systole, degrees	−0.083	0.595			
AH/ICW ratio in mid-systole, abs	0.034	0.826			
Leaflet coaptation					
Total-to-closed leaflet ratio, abs	−0.678	**<0.001**	−0.634 (−1.037 to −0.230)	−0.634	**0.003**

Possible predictors are presented with their corresponding regression coefficient and *P* value. Variables with $P < 0.10$ in univariate linear regression were subsequently entered into the multivariable linear regression model. Multicollinearity was always verified. Significant *P* values are indicated in **bold**.

Abbreviations as in Tables 1 and 3.

echocardiography data in AF and sinus rhythm, the present study provides unique insights into mitral annular dynamics in AF and the mechanisms underlying AFMR. It is demonstrated that blunting of the presystolic (atrial) annular narrowing is the predominant difference in annular dynamics between AF and sinus rhythm, significantly affecting mitral valve competence in AF. Although subtle differences in dynamics of nonplanarity angle and saddle-shape were appreciated, these were not significantly different between AF and sinus rhythm at any time point, nor independently associated with AFMR.

AFMR IMPROVEMENT FOLLOWING SINUS RHYTHM RESTORATION. Marked improvements in MR severity in patients who successfully maintained sinus rhythm after catheter ablation (5,25) or electric cardioversion (26) are generally thought to be mechanistically related to reverse LA remodeling, improving valve coaptation.

The present study now demonstrates that not LA remodeling (ie, LA volume index), but rather improved mitral annular dynamics that follow successful sinus rhythm restoration are implicated in the observed decreases in EROA. Indeed, the decrease in MR severity at 6 weeks was primarily assigned to the recovery in presystolic annular motion, not to LA or LV remodeling. Enhanced presystolic annular narrowing sets the stage for a smaller annular area throughout systole, thereby decreasing the leaflet area needed to adequately close the mitral valve orifice. As such, improved mitral annular dynamics in sinus rhythm optimize the total-to-closed leaflet area ratio, improving mitral valve coaptation and AFMR (**Central Illustration**). Importantly, the recovery in annular dynamics 6 weeks after sinus rhythm restoration was even larger in the subgroup with significant AFMR (EROA ≥0.20 cm^2), paralleling improved annular-leaflet balance that correlated with EROA. It is conceivable that a recovery of atrial contractile function parallels this normalization of annular function. There is extensive evidence from the earliest history of AF cardioversion of a delayed return of LA mechanics (27-30).

CLINICAL IMPLICATIONS. The optimal management of AFMR has yet to be established. This study acknowledges the role of mitral annular dysfunction in the pathophysiology of AF and AFMR and its potential reversibility after sinus rhythm restoration. Hence, for management of AFMR, AF therapy should ideally extend beyond anticoagulation and rate-control therapy, focusing on preserving sinus rhythm early in light of annular anatomical and mechanical remodeling. From the present results, a gradual recovery of presystolic annular dynamics is considered to be the key mechanism for MR improvement by restoring the annular-leaflet imbalance. In addition, our findings suggest a potential role for therapies enhancing mitral leaflet adaptation to improve the annular-leaflet imbalance in AFMR. This

FIGURE 3 Longitudinal Change in Presystolic Annular Dynamics, Total-to-Closed Leaflet Area, And EROA

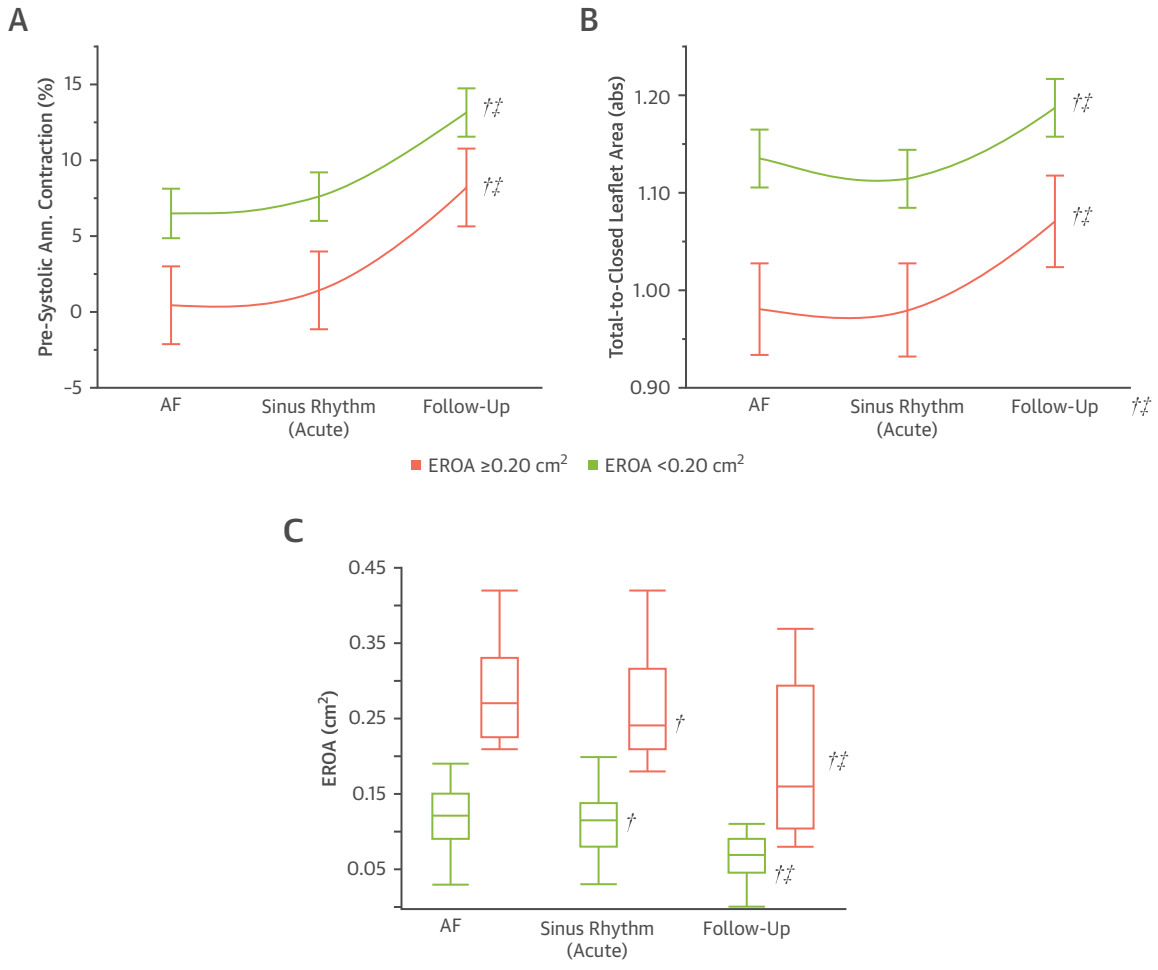

Presystolic annular dynamics and leaflet coaptation (total-to-closed leaflet area) were significantly worse in patients with EROA ≥0.20 cm^2 at each point in time **(A, B)**. Nevertheless, the recovery in annular dynamics was larger in this subgroup, paralleling a significant decrease in EROA **(C)**. AF = atrial fibrillation; EROA = effective regurgitant orifice area. †$P < 0.05$ vs AF; ‡$P < 0.05$ vs sinus rhythm.

should be a subject of further research (31,32). The recently published EAST (Early Treatment of Atrial Fibrillation for Stroke Prevention; NCT01288352) trial (33) showed significantly better cardiovascular outcomes after early rhythm-control therapy in subjects with early AF and cardiovascular conditions, compared with usual care. Whether this is partially attributable to a reduction in MR severity among nearly one-half of patients with concomitant valvular disease is unknown.

STUDY LIMITATIONS. Quantification of MR severity in AFMR is challenging because the regurgitant jet is often dispersed along the coaptation line. Consequently, calculation of EROA by the 2D proximal flow convergence method is known to underestimate true MR severity in AFMR because of its nonhemispheric convergence flow area. EROA was therefore measured by direct planimetry of the 3D vena contracta area to overcome this limitation.

The recovery in presystolic annular dynamics was independently linked to the reduction in EROA, as opposed to changes in LA volume index or atrial booster pump function. The relative short time of follow-up in this study could hamper the independent association between anatomical or mechanical LA reverse remodeling and changes in EROA.

Patients had no implantable cardiac devices. As such the exact AF burden (number and length of individual episodes) could not be assessed and subclinical AF episodes may have gone undetected. However, this largely reflects the clinical reality in most patients with AFMR.

CENTRAL ILLUSTRATION **Annular Dynamics and Leaflet (Mal)coaptation During AF and 6 Weeks After Sinus Rhythm Restoration**

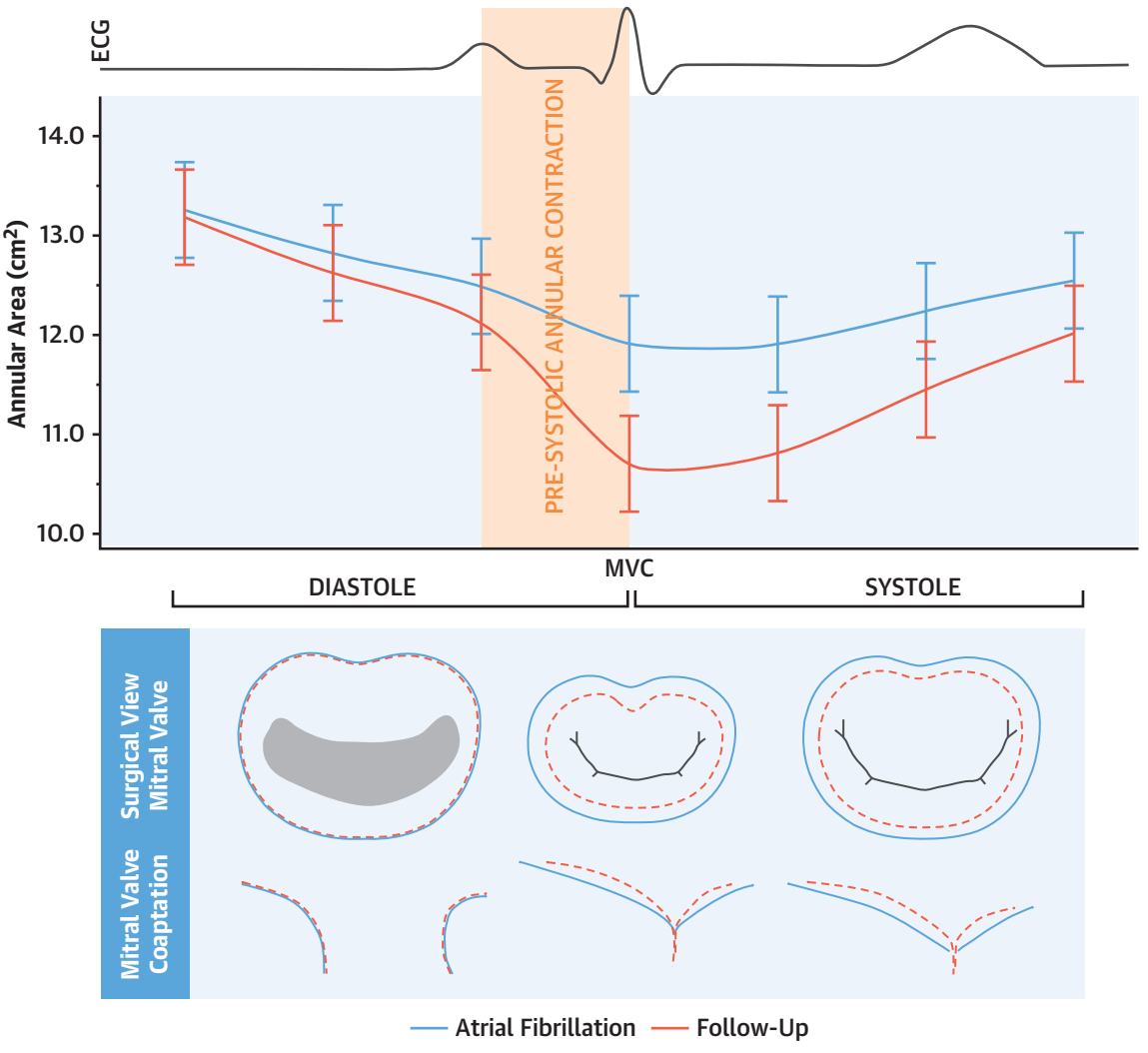

Deferm, S. et al. J Am Coll Cardiol Img. 2022;15(1):1–13.

Mitral annular dynamics are blunted during persistent AF and immediately after sinus rhythm restoration, particularly during pre-systole. Regained presystolic annular contraction improves valve coaptation throughout systole and decreases MR severity, regardless of LA size. AF = atrial fibrillation; ECG = electrocardiography; LA = left atrial; MR = mitral regurgitation; MV = mitral valve; MVC = mitral valve closure.

CONCLUSIONS

Mitral annular dynamics are impaired in AF, with predominant blunting of presystolic annular narrowing (loss of atrial contraction) which contributes to leaflet malcoaptation and AFMR. Sinus rhythm restoration allows gradual recovery of annular dynamics, particularly in the presystolic annular contraction phase. Improved annular dynamics in sinus rhythm decrease AFMR severity by improving the annular-leaflet imbalance, regardless of global LA remodeling.

ACKNOWLEDGMENT The authors acknowledge Mr Christof Palmers for his help with the data processing.

FUNDING SUPPORT AND AUTHOR DISCLOSURES

Drs Deferm and Vandervoort are researchers for the Limburg Clinical Research Program UHasselt-ZOL-Jessa, supported by the foundation

Limburg Sterk Merk, Hasselt University, Ziekenhuis Oost-Limburg, and Jessa Hospital. Drs Deferm and Vandervoort are part of an Interreg project (Poly-Valve) aimed at providing tailor-made heart valve prostheses using coated biomedical polyurethane. Dr Verbrugge is supported by a Fellowship of the Belgian American Educational Foundation and by the Special Research Fund of Hasselt University (BOF19PD04). Dr Rega has been a consultant for Atricura and; LivaNova and has received research funding from Medtronic. Dr Thomas has been a consultant for and has received honoraria from Edwards, Abbott, GE, and Caption Health; and his spouse is an employee of Caption Health. All other authors have reported that they have no relationships relevant to the contents of this paper to disclose.

ADDRESS FOR CORRESPONDENCE: Dr Pieter M. Vandervoort, Department of Cardiology, Ziekenhuis Oost-Limburg, Schiepse Bos 6, 3600 Genk, Belgium. E-mail: pieter.vandervoort@zol.be.

PERSPECTIVES

COMPETENCY IN MEDICAL KNOWLEDGE: Presystolic annular contraction is impaired during persistent AF and recovers gradually after sinus rhythm restoration. This recovery in annular dynamics improves annular-leaflet imbalance in AFMR, which is key for a decrease in regurgitation severity.

TRANSLATIONAL OUTLOOK: Presystolic annular dynamics are impaired in persistent AF but can gradually recover after sinus rhythm restoration. The net result is improved leaflet coaptation, and, thus a decrease in mitral regurgitation severity, regardless of global LA remodeling.

REFERENCES

1. Deferm S, Bertrand PB, Verbrugge FH, et al. Atrial functional mitral regurgitation: *JACC* review topic of the week. *J Am Coll Cardiol*. 2019;73:2465–2476.

2. Deferm S, Dauw J, Vandervoort PM, Bertrand PB. Atrial functional mitral and tricuspid regurgitation. *Curr Treat Options Cardiovasc Med*. 2020;22:30.

3. Kagiyama N, Mondillo S, Yoshida K, Mandoli GE, Cameli M. Subtypes of atrial functional mitral regurgitation: imaging insights into their mechanisms and therapeutic implications. *J Am Coll Cardiol Img*. 2020;13:820–835.

4. Tanimoto M, Pai RG. Effect of isolated left atrial enlargement on mitral annular size and valve competence. *Am J Cardiol*. 1996;77:769–774.

5. Gertz ZM, Raina A, Saghy L, et al. Evidence of atrial functional mitral regurgitation due to atrial fibrillation: Reversal with arrhythmia control. *J Am Coll Cardiol*. 2011;58:1474–1481.

6. Tang Z, Fan YT, Wang Y, Jin CN, Kwok KW, Lee APW. Mitral annular and left ventricular dynamics in atrial functional mitral regurgitation: a three-dimensional and speckle-tracking echocardiographic study. *J Am Soc Echocardiogr*. 2019;32:503–513.

7. Machino-Ohtsuka T, Seo Y, Ishizu T, et al. Novel mechanistic insights into atrial functional mitral regurgitation—3-dimensional echocardiographic study. *Circ J*. 2016;80:2240–2248.

8. Silbiger JJ. Mechanistic insights into atrial functional mitral regurgitation: far more complicated than just left atrial remodeling. *Echocardiography*. 2019;36:164–169.

9. Silbiger JJ. Anatomy, mechanics, and pathophysiology of the mitral annulus. *Am Heart J*. 2012;164:163–176.

10. Levack MM, Jassar AS, Shang EK, et al. Three-dimensional echocardiographic analysis of mitral annular dynamics: Implication for annuloplasty selection. *Circulation*. 2012;126:7–8.

11. Chen TE, Ong K, Suri RM, et al. Three-dimensional echocardiographic assessment of mitral annular physiology in patients with degenerative mitral valve regurgitation undergoing surgical repair: comparison between early- and late-stage severe mitral regurgitation. *J Am Soc Echocardiogr*. 2018;31:1178–1189.

12. January CT, Wann S, Alpert JS, et al. 2014 AHA/ACC/HRS guideline for the management of patients with atrial fibrillation: a report of the American College of Cardiology/American Heart Association Task Force on Practice Guidelines and the Heart Rhythm Society. *J Am Coll Cardiol*. 2014;64:2246–2280.

13. Lang RM, Badano LP, Mor-Avi V, et al. Recommendations for cardiac chamber quantification by echocardiography in adults: an update from the American society of echocardiography and the European association of cardiovascular imaging. *J Am Soc Echocardiogr*. 2015;28:1–39.e14.

14. Kusunose K, Yamada H, Nishio S, et al. Index-beat assessment of left ventricular systolic and diastolic function during atrial fibrillation using myocardial strain and strain rate. *J Am Soc Echocardiogr*. 2012;25:953–959.

15. Voigt J-U, Pedrizzetti G, Lysyansky P, et al. Definitions for a common standard for 2D speckle tracking echocardiography: consensus document of the EACVI/ASE/Industry Task Force to Standardize Deformation Imaging. *J Am Soc Echocardiogr*. 2015;28(2):183–193.

16. Zoghbi WA, Adams D, Bonow RO, et al. Recommendations for noninvasive evaluation of native valvular regurgitation: a report from the American Society of Echocardiography developed in collaboration with the Society for Cardiovascular Magnetic Resonance. *J Am Soc Echocardiogr*. 2017;30:303–371.

17. Zeng X, Levine RA, Hua L, et al. Diagnostic value of vena contracta area in the quantification of mitral regurgitation severity by color doppler 3D echocardiography. *Circ Cardiovasc Imaging*. 2011;4:506–513.

18. Grewal J, Suri R, Mankad S, et al. Mitral annular dynamics in myxomatous valve disease: new insights with real-time 3-dimensional echocardiography. *Circulation*. 2010;121:1423–1431.

19. Salgo IS, Gorman JH, Gorman RC, et al. Effect of annular shape on leaflet curvature in reducing mitral leaflet stress. *Circulation*. 2002;106:711–717.

20. Glasson JR, Komeda M, Daughters GT, et al. Most ovine mitral annular three-dimensional size reduction occurs before ventricular systole and is abolished with ventricular pacing. *Circulation*. 1997;96 9 Suppl:II 115–II-122; discussion II 123.

21. Timek TA, Lai DT, Dagum P, et al. Ablation of mitral annular and leaflet muscle: effects on annular and leaflet dynamics. *Am J Physiol Heart Circ Physiol*. 2003;285:H1668–H1674.

22. Timek TA, Lai DT, Tibayan F, et al. Atrial contraction and mitral annular dynamics during acute left atrial and ventricular ischemia in sheep. *Am J Physiol Heart Circ Physiol*. 2002;283:H1929–H1935.

23. Timek T, Dagum P, Lai DT, et al. The role of atrial contraction in mitral valve closure. *J Heart Valve Dis*. 2001;10:312–319.

24. Ring L, Dutka DP, Wells FC, Fynn SP, Shapiro LM, Rana BS. Mechanisms of atrial mitral regurgitation: insights using 3D transoesophageal echo. *Eur Heart J Cardiovasc Imaging*. 2014;15:500–508.

25. Nishino S, Watanabe N, Ashikaga K, et al. Reverse remodeling of the mitral valve complex after radiofrequency catheter ablation for atrial fibrillation: a serial 3-dimensional echocardiographic study. *Circ Cardiovasc Imaging*. 2019;12:e009317.

26. Dell'Era G, Rondano E, Franchi E, Marino PN. Atrial asynchrony and function before and after electrical cardioversion for persistent atrial fibrillation. *Eur J Echocardiogr*. 2010;11:577–583.

27. Manning WJ, Silverman DI, Katz SE, et al. Impaired left atrial mechanical function after cardioversion: relation to the duration of atrial fibrillation. *J Am Coll Cardiol*. 1994;23:1535–1540.

28. Iuchi A, Old T, Fukuda N, et al. Changes in transmitral and pulmonary venous flow velocity patterns after cardioversion of atrial fibrillation. *Am heart J*. 1996;131(2):270–275.

29. Mattioli AV, Sansoni S, Lucchi GR, Mattioli G. Serial Evaluation of left atrial dimension after cardioversion for atrial fibrillation and relation to atrial function. *Am J Cardiol*. 2000;85:832–836.

30. Thomas L, Mckay T, Byth K, Marwick TH. Abnormalities of left atrial function after cardioversion: an atrial strain rate study. *Heart*. 2007;93:89–95.

31. Bartko PE, Dal-Bianco JP, Guerrero JL, et al. Effect of losartan on mitral valve changes after myocardial infarction. *J Am Coll Cardiol*. 2017;70:1232–1244.

32. Kim DH, Heo R, Handschumacher MD, et al. Mitral valve adaptation to isolated annular dilation. insights into the mechanism of atrial functional mitral regurgitation. *J Am Coll Cardiol Img*. 2019;12:665–677.

33. Kirchhof P, Camm AJ, Goette A, et al. Early rhythm-control therapy in patients with atrial fibrillation. *N Engl J Med*. 2020;383:1305–1316.

KEY WORDS atrial fibrillation, atrial functional mitral regurgitation, electric cardioversion, mitral annulus, mitral regurgitation, three-dimensional echocardiography

APPENDIX For supplemental figures and tables, please see the online version of this paper.